Abrupt transitions between gyroscopic and internal gravity waves: the mid-latitude case

HANS VAN HAREN

Royal Netherlands Institute for Sea Research (NIOZ), PO Box 59,
1790 AB Den Burg, The Netherlands
hansvh@nioz.nl

The large-scale vertical density stratification, represented by buoyancy frequency N, is generally very stable in the upper half of the ocean, and relatively weak in the lower half. However, closer inspection of density profiles demonstrates steps rather than a smooth increase with depth. As is demonstrated here using Richardson number, geostrophic balance and slantwise convective mixing arguments, these layers have a limited set of minimum, weak stratification, N-values N_{min} indicating the transition between stably stratified and convective 'homogeneous' layers. Adopting the viewpoint that the transition occurs for neutral stability in the direction of Earth's rotation Ω instead of gravity g, three discrete states are hypothesized for mid-latitudes: (i) $N_{min} = 2f_h$ under linear stability conditions, (ii) $N_{min} = f_h(|\varphi| < 45°)$ and (iii) $N_{min} = 4f_h$, both under nonlinear stability, where horizontal component $f_h = 2\Omega \cos \varphi$ at latitude φ. The N_{min} are not in terms of inertial frequency $f = 2\Omega \sin \varphi$, because the effect of f_h is the tilting of vortex tubes away from the local vertical in the direction of Ω. The above explains very well deep-ocean North-Atlantic and Mediterranean observations on transitions in conductivity-temperature with depth profiles, inertial polarization and near-inertial shear. The latter peaks at sub-inertial $0.97f$, which is associated with the lower inertio-gravity wave limit for $N_{min} = 4f_h$, thereby stressing the importance of f_h for the dominant physics associated with mixing in the ocean.

1. Introduction

Deep-ocean current meter observations from the Mediterranean Sea show an abrupt buoyancy frequency (N) dependence of horizontal current polarization at near-inertial frequencies $\sigma = f$. Here, $f = 2\Omega \sin \varphi$ represents the local vertical component of the Earth's rotational vector Ω at latitude φ. This polarization varies from the familiar near-circular polarization, when $N > f$, 'stratified' waters, to near-rectilinear polarization, when $N = 0$, 'homogeneous' waters (van Haren & Millot 2004). Such varying polarization has a large impact on the vertical shear of horizontal currents, which is generally found to be dominant at f outside internal tide generation areas (Figure 1). Shear at f is important, because of the short vertical scale of near-inertial (wave) motions. The shear magnitude is relevant for destabilization of the commonly stable large-scale vertical density stratification in the ocean. As a result, a transition from circular shear, with magnitude constant with time, to rectilinear shear, with magnitude varying with time at the inertial period, thus implies a radical change from diapycnal shear-induced to convective mixing.

This change in polarization (figure 2) has been attributed (van Haren & Millot 2004) to a relatively large influence of the horizontal component of the Coriolis
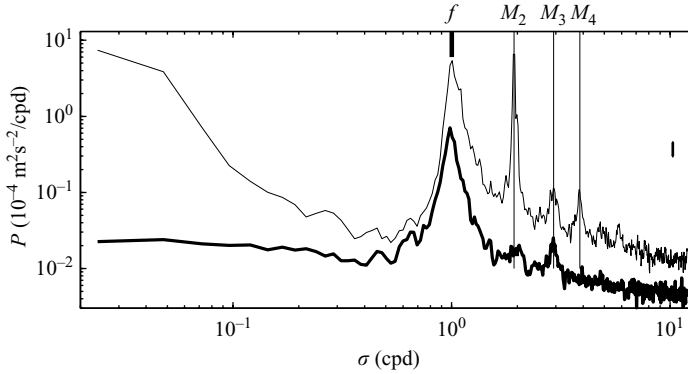
FIGURE 1. Smoothed spectra from 1.5 years of moored 75 kHz ADCP (acoustic Doppler current profiler)-data from the Canary Basin (30°N, 23°W) of kinetic energy E_k (thin) and current difference (∼shear) over 30 m (thick; arbitrarily off-set vertically) observed around 1100 m. E_k is dominated by tidal, inertial and low-frequency currents, whilst shear only shows a large peak at f.

force $f_h = 2\Omega \cos\varphi$ in homogeneous waters, or equivalently, a dominant influence of reduced gravity on near-inertial wave motions in weakly, but sufficiently stratified waters. The transition not only affects shear and mixing, but also propagation of different types of internal inertio-gravity waves (IGW). Free propagating gyroscopic waves dominate in homogeneous waters and internal gravity waves dominate in stratified waters. These different waves have similar properties and are included in a single dispersion relation, but the former have phase and energy propagation in the same vertical direction whereas for the latter it is in opposing vertical directions (LeBlond & Mysak 1978). In addition to different propagating waves, waves at different frequencies can be trapped in differently stratified layers. Sub-inertial waves can be trapped in weakly stratified waters $N > f$ (Gerkema & Shrira 2005b) whereas super-inertial waves can be trapped in homogeneous waters (van Haren 2006). In the latter paper it was argued that only waves at exactly $\sigma = f$ can always propagate from stratified to homogeneous layers and vice versa. However, the reason for the abruptness of the change in stratification between non-zero and zero N was not clear.

In this paper, some reason for the particular non-zero $N > f$ before transition to $N = 0$ is given, based on the gradient Richardson number balance. This is combined with an analogy of slanted convective plume dynamics (Marshall & Schott 1999; Straneo, Kawase & Riser 2002; Sheremet 2004) and thermal wind balance for a density-stratified ocean (e.g. Gill 1982). In particular, the shear effects of circular transient motions will be considered in addition to those of geostrophically balanced unidirectional 'constant' motions. Strong vertical motions in free convective plumes show vortex tubes tilted from the local vertical by f_h-terms, which are usually considered weak outside such areas. When f_h-terms affect near-inertial internal waves, strong vertical inertial currents are expected of aspect ratio 1, $w = O(u, v)$, see the Appendix. Here, (u, v, w) represent (east, north, vertical) current components.

2. Stratification variations

In the deeper half of the mid-latitude Western Mediterranean Sea (∼40°N), observations of currents $[u, v]$ in the horizontal plane show near-circular inertial motions that change to near-rectilinear ones without appreciable attenuation of
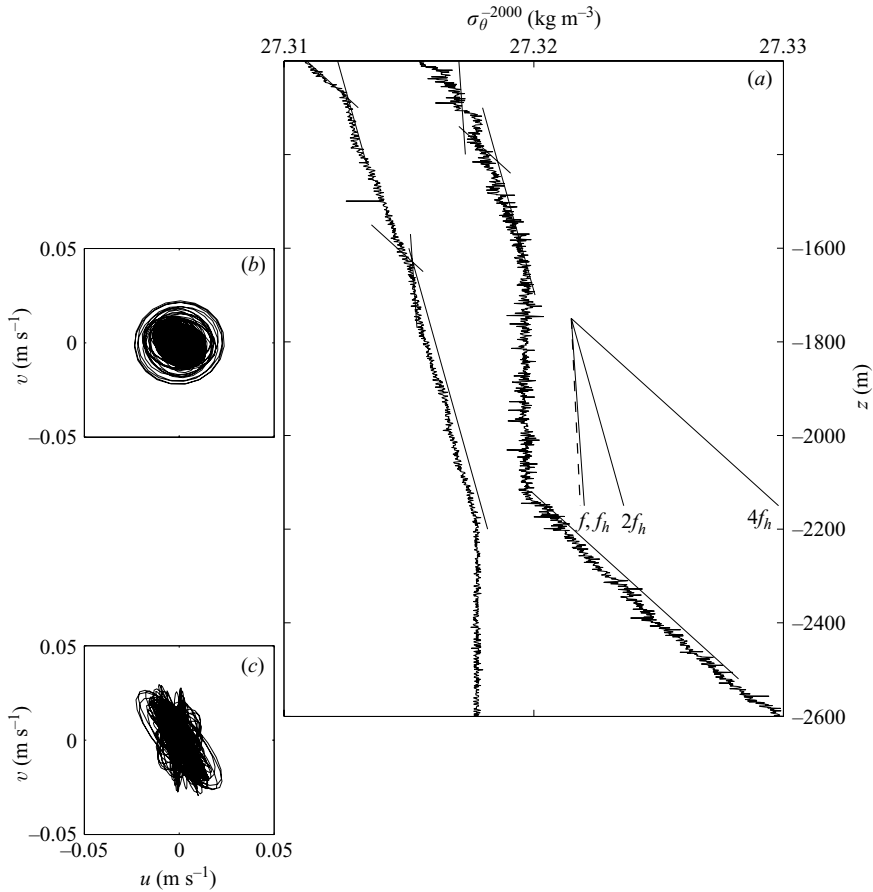
FIGURE 2. (a) Examples of 1-m vertical bin averaged density anomaly versus depth obtained in the Algerian Basin of the Western Mediterranean Sea at 38.5°N, 8°E in 1997 (left-hand profile) and at 40°N, 6°E in 2006 (right-hand profile). The CTD-data are referenced to 2000 m (ρ_{2000} -1008.650 kg m^{-3}). The straight sloping lines represent density stratification in layers ± 200 m around the reference depth for $N = f$ (dashed), f_h ($\approx 1.25f$ here, solid), $2f_h$ ($\approx 2.5f$, solid), $4f_h$ ($\approx 5f$, solid). Hodographs of band-pass filtered horizontal inertial currents measured in 1997 at (b) 1800 and (c) 2700 m.

amplitude. This change is found where the relatively large-scale stratification changes with depth from $N = 2.5 \pm 0.5f$ to $N = 0$ (van Haren & Millot 2004; Figure 2 here). Vertical density (ρ) stratification is represented by buoyancy frequency $N(z) = (-g/\rho)(\partial \rho'/\partial z)^{1/2}$, where g denotes the acceleration due to gravity, and ρ' the density relative to the ambient value. A vertical scale $\Delta z > 100$ m is considered 'large-scale' here. The $N = 0$ represents homogeneous waters, presumably following convective overturning, and it is determined to within an error of $< 0.8f$. These N-values and errors are computed using SeaBird 911 CTD (conductivity-temperature-depth) data and a vertical window equivalent to 100 dbar pressure change (van Haren & Millot 2006). Part of the error, especially in homogeneous waters, is due to the imperfect resolution of temperature variations equivalent to those of the adiabatic lapse rate. In stratified waters, an unknown part of the error is due to the mismatch in scales between internal wave motions and variations in 'background stratification'.
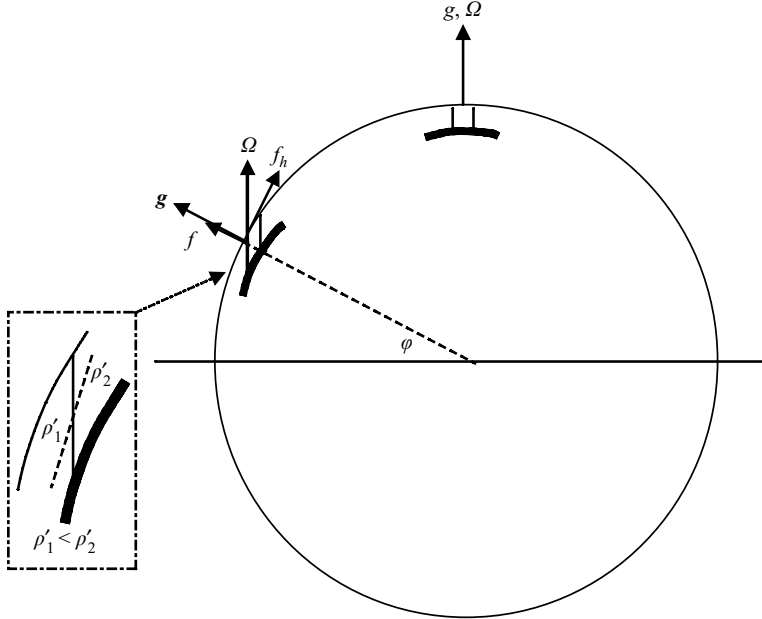
FIGURE 3. Sketch of relative isopycnals with respect to the direction of the Earth's rotational vector and the correspondence with gravity ($//f$, $\perp$ local horizontal 'f-plane'). Isopycnals are indicated by the thin solid line when neutral stability $//\boldsymbol{\Omega}$ and by the dashed line when creating stable stratification along $\boldsymbol{\Omega}$ (see insert).

Here we seek an explanation for this particular apparent minimum non-zero stratification bordering layers of $N = 0$ (Figure 2). This is relevant for better understanding of internal wave propagation as gravity waves ($N > f$) and as gyroscopic waves ($N = 0$), as well as for better understanding of internal wave-induced mixing. In the following, we assume that dominant large-scale $\Delta z > 100$ m shear is found at sub-inertial frequencies and small-scale $\Delta z = 10$ m shear at or very near $\sigma = f$, the frequency that is most transparent across transitions between stratified and homogeneous layers (Appendix; some further details in van Haren 2006).

2.1. Hypothesis for slantwise shear balance

In analogy with convective plume dynamics (reviewed by Marshall & Schott 1999), we search for minimum $N(z) = N_{min}$ associated with neutral stability *in the direction of the Earth's rotational vector* (figure 3). This is called slant-convection in plume dynamics or 'tilted Taylor ink wall' (Sheremet 2004) as convection is not in the direction of gravity, except at $|\varphi| = 90°$ where $\boldsymbol{\Omega}$ and $\boldsymbol{g}$ are parallel.

The hypothesis is that a gyroscopic inertial wave propagates along $\boldsymbol{\Omega}$ when stratification is weak, $N \leqslant N_{min}$, so that planes of constant density are parallel to, or more vertical than, the Earth's angular momentum vector. When $N = N_{min}$, 'diapycnal' mixing no longer exists and dominant (slantwise) 'mixing' along the rotational vector becomes isopycnal, or for still weaker $N < N_{min}$, convectively unstable.

Equivalently, it is hypothesized that only for $N > N_{min}$, does sufficient stability exist that inertial gravity waves and shear can exist. Given the large angle between $\boldsymbol{\Omega}$ and $\boldsymbol{g}$ at mid-latitudes, it is expected that the minimum stratification will differ substantially from zero, so that the transition between inertial internal gravity and gyroscopic

waves will be abrupt, including a sudden change between diapycnal shear-induced and convective mixing regimes and an abrupt vertical variation in density profiles.

The above hypothesis is based on the following empirical first-order balances. The transition of neutral stability in the direction of $\boldsymbol{\Omega}$ occurs for (e.g. Marshall & Schott 1999),

$$|N/N_h|^2 = 1/\tan\varphi = f_h/f, \qquad (2.1)$$

where $N_h^2 = (g/\rho)(\partial\rho'/\partial y)$, y denotes the local horizontal coordinate in the meridional direction. The same horizontal density gradient but of opposite sign, $-N_h^2$, just cancels out the slantwise tilting of planes of constant momentum owing to f_h and the familiar vertical buoyancy oscillation is retrieved (Straneo *et al.* 2002). Horizontal density gradients in the zonal x-direction are not relevant here. They may adopt an arbitrary value. For $|\varphi| < 45°$, (2.1) implies an aspect ratio > 1.

Next, the vertically slanted isopycnals are attributed to a thermal wind or geostrophic balance between the *horizontal* density gradient in the meridional direction and the *vertical* shear in the zonal direction,

$$f\,\partial u/\partial z = N_h^2, \qquad (2.2)$$

which will be established after a sufficiently long time $t > 1/f$. Equation (2.2) is valid for all latitudes, except $|\varphi| < 1.5°$ for which the complete thermal wind balance in spherical coordinates should be considered (Colin de Verdière & Schopp 1994).

The balance (2.2) can be recast as one relating the vertical density gradient and the magnitude of the shear vector $\boldsymbol{S} = (\partial u/\partial z,\ \partial v/\partial z)$,

$$|N_h^2| = N^2\tan\varphi = f|\boldsymbol{S}|, \qquad (2.3a)$$

or,

$$N^2 = f_h|\boldsymbol{S}|, \qquad (2.3b)$$

provided shear magnitude is constant with time, as is assumed for density gradients. Equation (2.3) indicates a balance between vertical stratification and shear owing to a tilt from the vertical of f_h. For the present purpose it is assumed that (2.3) is valid in different layers with different N and $|\boldsymbol{S}|$. This leaves a matching problem between layers to be solved as well as a set-up problem for slow variations with time within a layer.

Constant shear magnitude with time is typical for unidirectional flows varying in amplitude with depth, as in steady geostrophic flows. It is also typical for purely horizontally circular oscillatory flows varying in amplitude or phase with depth, as in inertially oscillating transients $\propto\exp(-ift)$ following a geostrophic adjustment. For both flows, the shear magnitude varies slowly with time $\gg 1/f$, fulfilling the requirement for the validity of (2.2). However, circular flow is not uniquely along contours of constant density as required for (2.2), so that, in fact, the balance (2.3) reflects vertical exchange rather than density-driven flow for such oscillatory sheared motions, as outlined below.

The argument is that when geostrophic shear (2.2) is set up, the associated stratification N in (2.3) can support internal gravity waves. Such waves naturally provide internal wave shear, which, however, cannot exist if the geostrophic shear in (2.2) is marginally stable and any additional shear induces diapycnal mixing. That means transients associated with any geostrophic adjustment process and having the same amplitude as the geostrophic current (e.g. Gill 1982) directly destroy any stratification associated with slanted isopycnals, if marginally stable. Therefore, we consider a scale separation for the shear, with large vertical scales for geostrophically

balanced flow and short vertical scales for transients, which are at f, near the small-scale lower limit of the internal gravity wave band (e.g. Leaman & Sanford 1975). It is hypothesized that over the large scale, the geostrophically balanced density variation is equivalent to the sum of a thin layer of larger density variation and a layer of smaller density variation, thus providing 'steps'.

The problem to be solved is the onset in the geostrophic adjustment problem. The set-up is fast, $O(1/f)$, initially with an overshoot within one inertial period. In shelf seas, and presumably in the ocean as well, the response is not a baroclinic wave, but, through a horizontal boundary condition, a barotropic response so that the transients show π-phase-difference across the largest stratification (Millot & Crépon 1981). In contrast with the classic geostrophic balance, (2.2), of a steady unidirectional flow, which demonstrates a shear relative to an arbitrary level, the maximum shear associated with inertial motions is found centred by the stratified layer and, imperatively, shows π-phase-difference or maximum shear in at least one component. Owing to the circular character of inertial motions and shear, this implies a similar shear in the other (along) current direction.

The suggestion is that geostrophic adjustment of stratification following or bordering free slant-wise convection is balanced, perhaps initially by linear geostrophic shear, but most probably in equilibrium added by or consisting of 'transient' inertial wave shear in small layers. From a stability perspective, it is impossible for the stratification to support the linear marginally balancing geostrophic shear and the shear imposed by the transients at the same time, unless the shear is somehow partitioned at the different vertical scales.

2.2. *Minimum stratification related to marginal linear stability*

The above quasi-permanent destabilizing shear can be (just) permanently supported by stable stratification when the gradient Richardson number,

$$Ri = N^2/|S|^2 \geqslant 0.25, \tag{2.4}$$

a threshold condition below which mixing can occur (Miles 1961; Howard 1961), or equivalently, a condition for marginal (linear) stability. Any weaker stable stratification cannot support the destabilizing shear, so that the water column must be homogenized. Combining (2.3) and (2.4) yields the maximum shear for linear stability maintaining thermal wind balance (2.2) following slantwise convection,

$$|S|_{max,lin} = 4f_h. \tag{2.5a}$$

Likewise, if we take the instability limit $Ri \uparrow 0.25$ as a viewpoint, we find the associated minimum stratification,

$$N = N_{min,lin} = 2f_h. \tag{2.5b}$$

Note that we cannot use the viewpoint of stability to find the stratification limit, as this would give maximum N, or the viewpoint of instability to find the shear limit, as this would give minimum $|\delta|$. Also note that the above transitional N and $|S|$ are expressed in terms of f_h, rather than f.

$N_{min,lin}$ shows a latitudinal variation (figure 4), which in the Mediterranean Sea almost exactly equals the observed stratification above the large deep homogeneous layer: $f_h = 1.25f$ at $|\varphi| = 38.5°$ so that $N_{min,lin} = 2.5f$, well within the error of the observed value. This suggests that the Earth's rotation is entirely responsible for the maintenance of the non-zero stratification between $z \approx -1300$ and -2000 m (figure 2). For this range, the least-squares fit to the data of the left-hand profile varies less than 5% from the $2f_h$-slope. In turn, this marginal stable stratification, in fact, evidences
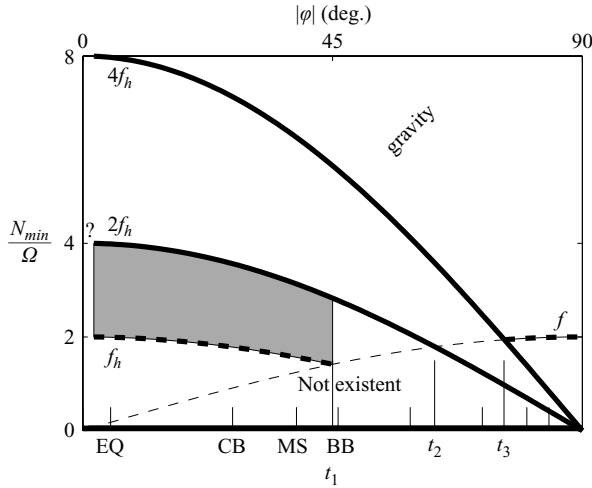
FIGURE 4. Latitudinal dependence of various minimum stratifications when neutral stability is precisely along $\boldsymbol{\Omega}$, associating with the meridional thermal wind balance: linear stability resulting in (2.5b), nonlinear stability resulting in (2.7a) and maximum linear stability shear under the condition of nonlinear stability resulting in (2.8). Internal gravity waves occur above the heavy solid curves (2.8), (2.5b), and can occur in the shaded transition area between (2.5b) and (2.7a) at $|\varphi| < 45°$. Stratification and waves are non existent in the white area below (2.5b) and above $N = 0$ (the latter supporting gyroscopic waves). Three transitional latitudes exist: $|\varphi_{t1}| = 45°$ above which $N_{min,nl} = f_h < f$, $|\varphi_{t2}| = $ arc $\tan(2) \approx 63.4°$ above which $N_{min,lin} = 2f_h < f$, $|\varphi_{t3}| = $ arc $\tan(4) \approx 75.9°$ above which $N_{min,max} = 4f_h < f$. EQ denotes the complex near-equatorial region CB. Canary Basin; MS, Mediterranean Sea BB; Bay of Biscay.

geostrophic adjustment following convective overturning along paths that are slanted towards the vertical (by f_h). Apparently, (2.5) and the underlying hypothesis can be valid for a small part of the watercolumn, despite an overall surface–bottom density difference that would result in a very stable $N \gg N_{min,lin}$.

The result is, as near-circular horizontal f-plane inertial motions always require stratification for support, and, furthermore, because $N_{min,lin} > f$ for mid-latitudes $|\varphi| < 63.4°$, the effective wave propagation vectors in weakly stratified ($\sim g$) and homogeneous ($\sim \boldsymbol{\Omega}$) waters still differ largely (Appendix). Hence, the transition is abrupt between gyroscopic and internal gravity inertial waves there, just like the linearly stable stratification (figures 2 and 5).

2.3. Minimum stratification related to marginal nonlinear stability

Naturally, weaker shears than in (2.5a) can be supported by $N_{min,lin}$. Van Haren & Millot (2004) report roughly observed near-inertial $|\boldsymbol{S}| = 1 \pm 0.4f \approx 0.4N_{min,lin}$ across scale height $\Delta z = 900$ m, which cannot be in thermal wind balance according to (2.3). However, Abarbanel *et al.* (1984) suggest that a parallel shear flow in a fully three-dimensional stratified fluid is unstable for non-linear perturbations when,

$$Ri_{nl} < 1. \tag{2.6}$$

Such a flow may be associated with internal inertial 'transient' waves. Under such stability condition (2.6), we arrive in terms of thermal wind balance (2.3) at a different, smaller, minimum stratification and associated maximum shear,

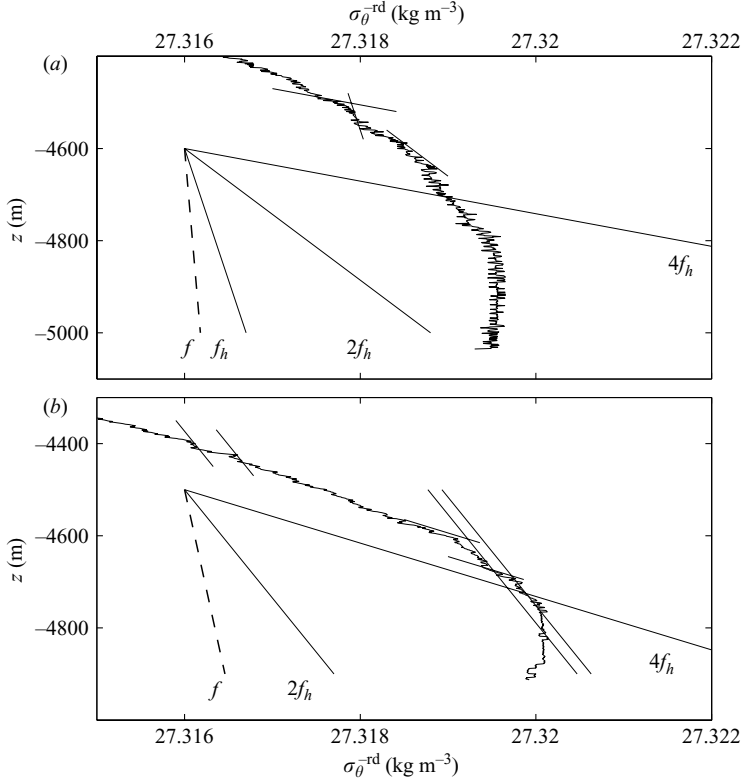$$N_{min,nl} = f_h = |\boldsymbol{S}|_{max,nl}, \tag{2.7a}$$

FIGURE 5. As figure 2 but focusing on near-bottom 600 m and for different mid-latitudes in the North Atlantic Ocean. The panels have the same scale, but reference density values vary (density anomaly values are arbitrary). (a) Canary Basin (27°, 23°W), (b) Bay of Biscay (46°, 5°W).

which relates to (2.5b) as,

$$N_{min,lin} = 2N_{min,nl}. \tag{2.7b}$$

This compares reasonably well with the above shear observation.

Such $N_{min,nl}$, and $N_{min,lin}$ forming a portion of it, are observed, but mainly in figures 2 and 5(a). Errors to the least-squares fits of small portions of data are less than 30%, the error to N across vertical scales of 100 m. This implies that short-scale variations to slowly varying $|S|$ are of second order, as required for (2.3). Possibly, (2.7) does not exist at $|\varphi| > 45°$ (figures 4, 5b), at which $N_{min,nl} < f$, or uniquely in a regime of gyroscopic waves and associated transition to vertical neutral stability. If we require a transition from gyroscopic to internal gravity waves we must at least allow both, hence part of the domain must show $N > f$.

2.4. *Maximum 'minimum' stratification*

A transition from linear to nonlinear stability may also result in an increase in local minimum stratification. When we consider preservation of maximum shear (2.5a) associated with linear stability under a condition of nonlinear stability, the minimum stratification becomes,
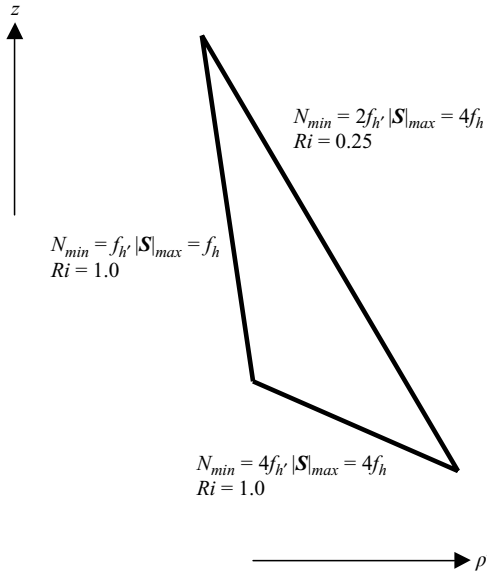
$$N_{min,max} = 4f_h. \tag{2.8}$$

FIGURE 6. Sketch of possible variations in density slopes, given neutral stability in the direction of $\boldsymbol{\Omega}$ for linear and nonlinear stabilities, together with the compensating larger slope for maximum shear under nonlinear stability (for $|\varphi| \leqslant 45°$).

In this case, the associated horizontal density gradient is no longer geostrophically balanced by the maximum shear associated with the marginal stability. The adaptation between the two stability conditions is by re-adjustment of the vertical length scale or layer thickness d, following a change in density variation $\Delta\rho$ or current variation Δu across d, since $Ri \propto d\Delta\rho/\Delta u^2$. The relationship between the three minimum stratifications and linear and nonlinear stability is sketched in figure 6.

In the deeper parts of the ocean, $z < -500$ m say, $N_{min,max}$ as in (2.8) is observed especially capping homogeneous layers and, like layers where $N = N_{min,lin}$ or $N_{min,nl}$ are matched, the correspondence with observations is well within instrumental errors, being < 20–30% (figures 2, 5). In particular, in figure 2 it is seen between -1300 and -1700 m (or -2100 m in the other profile) that $N_{min,lin}$ dominates the overall large-scale $\Delta z > 100$ m stratification whilst $N_{min,nl}$ and $N_{min,max}$ dominate in small layers within that range. Apparently, different linear and nonlinear flows occur in the same area to which different Ri are applicable.

The importance of (2.8) may be further appreciated, because it determines the layers of maximum inertial wave shear. It has been observed that the peak frequency of asymmetrically propagating near-inertial waves is red-shifted, with respect to f, to $0.97f$ in the Irminger Sea (van Haren 2006). This was explained as the trapping of sub-inertial waves in layers of $N > f$ (Gerkema & Shrira 2005b; van Haren 2006). Such peaks are also found in shear from other mid-latitudes (figure 7).

If the above minimum buoyancy frequency borders layers of $N = 0$, it implies a maximum extent of the IGW-band to sub-inertial frequencies $\sigma < f$, following (A 1) in the Appendix. Naturally, IGW can be extended to lower sub-inertial frequencies for smaller $N < f$, but then sub-inertial waves are not trapped (van Haren 2006). Associating maximum-linear shear with $N_{min,max}$ logically relates it with the lower IGW-limit (σ_{lo}, defined in (A 1) in the Appendix) at which the smallest wave scales are found. Apparently, such shear cannot exist undisturbed when any (non-)linear
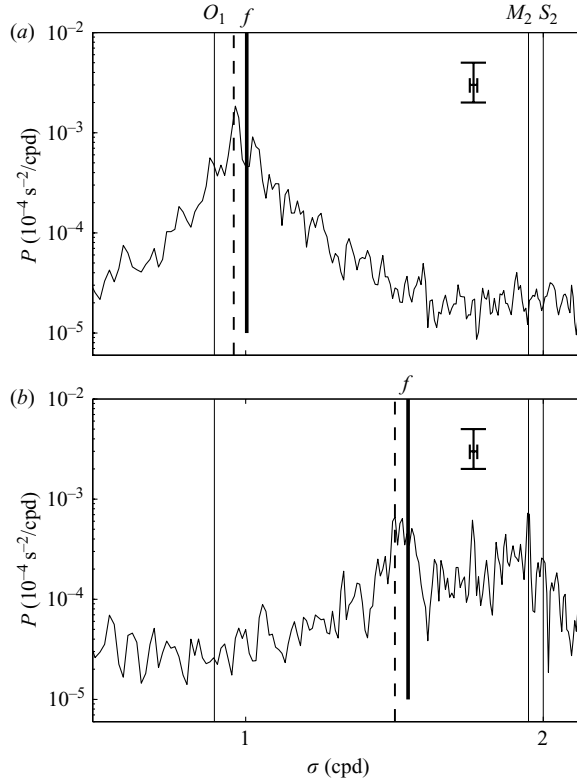
FIGURE 7. Nearly raw spectral details of shear computed from 75 kHz ADCP-data, (a) Canary Basin (30°N, 23°W, ∼1100 m), 19 months of data using $\Delta z = 30$ m, (b) Bay of Biscay (46°N, 5°W, ∼750 m), 11 months of data using $\Delta z = 48$ m. The vertical dashed line indicates $\sigma = 0.97f$.

instability exists, hence the association with (2.8). This σ_{lo}-relation with the f-peak is observed at all presently investigated mid-latitudes, for which f-scaled σ_{lo} remains more or less constant (figure 8). At $|\varphi| < 65°$, $\sigma_{lo} > 0.96f$, 1% within its maximum f-scaled value of 0.97 at the equator, but it drops rapidly to zero towards the poles.

Two remarks should be made here. First, (inertial) shear is in principle a much better quantity for verification of (2.8) than (inertial) current, as the latter commonly peaks at $\sigma > f$ for $N > f$, because freely propagating super-inertial waves exist beside trapped waves. Apparently, the latter have small scales yielding the dominating shear. In practice however, $O(10^{-4})$ s^{-1} shear is difficult to measure in the ocean with existing equipment across all relevant scales down to $\Delta z = 10$ m (Gargett *et al.* 1981). Mediterranean Sea data were obtained from current meters which were far enough apart vertically ($\gg 10$ m) that shear could not be properly determined across the relevant scales in the stratified layer. Hence, the current peak was taken from the homogeneous layer, thereby associating sub-inertial trapped waves in $N > f$ with propagating waves in $N < f$. Secondly, shear data in figure 8 were obtained from the depth range 1000–1500 m, whilst the stratification in figures 2 and 5 is from 1300 to 5000 m. This confirms the generalization of (2.5), (2.7) and (2.8) for the entire water column. Near-homogeneous layers just become smaller $O(1–10$ m) when $N \gg f$, which is generally found closer to the surface.
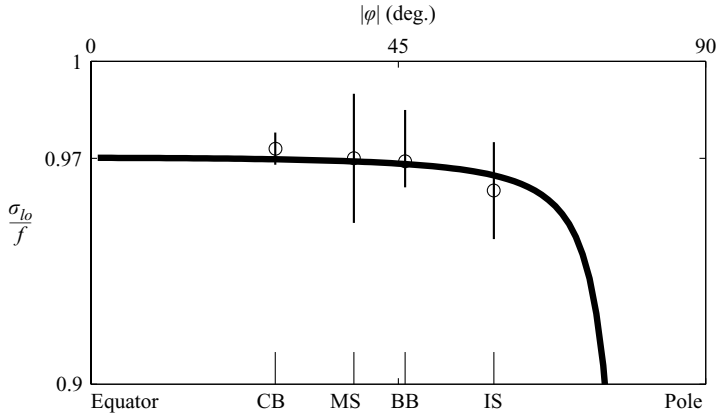
FIGURE 8. Sub-inertial peak-frequency observations (o) of 30–50 m vertical shear (of current for MS-data) from ~year-long 75 kHz ADCP-data. IS denotes Irminger Sea-data (59°, 33°W). The observations are compared with the theoretical lower IGW-limit (A 1) using $N = 4f_h$ (bold line). The vertical lines indicate standard errors, mostly related to spectral resolution. The longest time series (>1.5 years) is for CB-data.

3. Discussion

It is argued that a gradual transition between (inertial) internal gravity waves and gyroscopic waves cannot exist, except at the poles, on the Earth at the North Pole. This is in contrast with the suggestion of a smooth transition by van Haren & Millot (2004). Apparently, different waves obeying a joint dispersion relation can form an abrupt transition. Also, a smooth transition is not anticipated between near-inertial shear-induced and convectively driven mixing. Instead, transitions occur at discrete values for stratification, whereby the transitional values like (2.8) may either evidence trapping of near-inertial waves and shear or slanted convection, depending on the value of large-scale N. Minimum stratification is investigated in layers bordering layers of $N = 0$. Vertically homogeneous layers are due to a variety of processes, e.g. (i) horizontal advection following deep convection, (ii) rapid local IGW induced convection, or, (iii) double diffusion.

The given argumentation supported by deep-ocean CTD observations relates internal wave types to a transition across minimum stratification associated with neutral stability in the direction of the Earth's rotational vector. Weakly vertically stratified fluids are suggested to just support shear by linear and nonlinear motions. This seems possible as part of the shear is due to geostrophic motions whilst another part is due to inertial transients having different vertical scales. The finite frequency width of the inertial peak suggests nonlinear interaction with background flows. However, the precise transition between these different stability regimes requires further study, although both need non-zero stratification for support and horizontal inertial motions cannot be generated in surface-bottom homogeneous waters. Naturally, larger $N > N_{min}$ can exist that are not marginally balanced by destabilizing shear and which support a large range of internal gravity waves. It may be more interesting though to investigate layers where $N < N_{min}$.

Following the present data, such weak stratification is not initially expected higher up in the water column where generally much larger N and internal wave range are found. This is curious, because in all of the presented density profiles focusing on the deeper half of the water column, N_{min} rules $N(z)$. Of course we focused on this
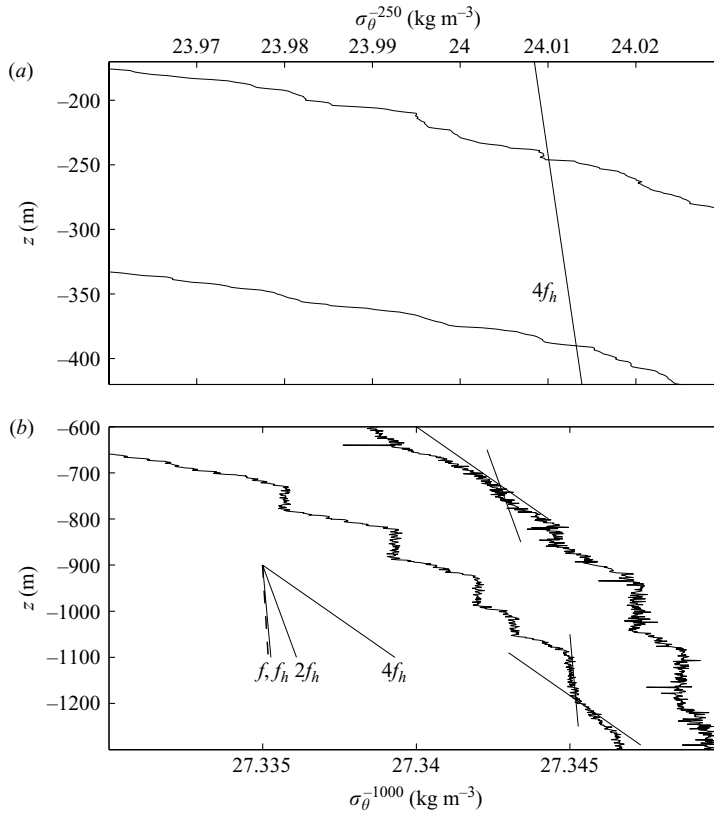
FIGURE 9. As figure 2 but focusing on upper half of the water column. (a) Near-surface part (referenced to 200 m), (b) upper-middle part.

part of the ocean where the slowest motions were expected possibly avoiding any disturbance by fast development $t < 1/f$, or by relative sub-inertial vorticity, but the presented ADCP-current and -shear spectra were from the mid-depth or upper-half of the water column.

Apparently, N_{min} can rule higher up as well, although observed more rarely than deep-down owing to smaller time- and length scales. Examples are given in figure 9, which are similar to near-surface (< 400 m) Labrador Sea data by Pickard as presented by Sheremet (2004) showing homogeneous layers 50–100 m thick and which are interpreted as evidence for slantwise convection. Although small N_{min}-layers become thinner and more rapidly relaxed under larger N, the effect of f_h on wave-propagation and slanted mixing thus even extends to apparently large N-layers. As a result, marginal stability induced by inertial waves and, in the deeper half, by geostrophic shear is more ubiquitous in the ocean than hitherto assumed. It is suggested that the stability state of the ocean is one in which turbulent diapycnal mixing may be relatively low, but slanted convection occurs regularly.

draft of the manuscript. Moored and CTD data were obtained during various projects partially supported by the Netherlands Organization for the advancement of scientific research, NWO, and Centre National de la Recherche Scientifique, CNRS.

Appendix. Inertio-gravity wave propagation and polarization

Inertio-gravity waves can propagate in the ocean interior when their frequency is in the range (e.g. LeBlond & Mysak 1978; Gerkema & Shrira 2005a),

$$\sigma_{lo} < \sigma < \sigma_{hi}, \tag{A1}$$

where

$$\sigma_{lo}^2 = s - (s^2 - f^2 N^2)^{1/2} < f^2, \quad \sigma_{hi}^2 = s + (s^2 - f^2 N^2)^{1/2} > N^2, \quad 2s = N^2 + f^2 + f_s^2,$$

elucidating the importance of the horizontal component of the Coriolis force, especially in the meridional direction as $f_s = f_h \sin\alpha$, α denoting the angle in the horizontal plane measured with respect to east. Besides the familiar short-waves at σ_{hi}, waves also have short scales at σ_{lo} (Saint-Guily 1970; Gerkema & Shrira 2005a), rendering them important for shear-induced mixing. In the limit of large buoyancy frequency $N >> f$ and for waves in the direction $\alpha = 0$ supported by any $N > f$, (A 1) reduces to the traditional internal gravity wave range $f \leqslant \sigma \leqslant N$. However, internal waves can also exist in homogeneous waters in the limit $N = 0$, for which (A 1) reduces to $0 \leqslant \sigma \leqslant 2\Omega$ ($\alpha = \pi/2$): gyroscopic waves.

In principle, there is and overlap $f \leqslant \sigma \leqslant 2\Omega$ between the ranges for the above two limits of N, but in practice only strict-inertial waves $\sigma = f$ can always propagate freely through stratification arbitrarily varying with depth as the gyroscopic wave range is in fact $0 \leqslant \sigma \leqslant (f^2 + f_s^2)^{1/2}$, which equals $[0, 2\Omega]$ for $\alpha = \pi/2$, but $[0, f]$ for $\alpha = 0$. Like internal gravity waves that propagate on cones around $\boldsymbol{g}$, the propagation planes for gyroscopic waves lie on cones around $\boldsymbol{\Omega}$ (LeBlond & Mysak 1978). These two vectors are separated by an angle $(\pi/2 - \varphi)$, so that the propagation planes of gyroscopic and internal gravity waves differ widely at mid- and low-latitudes. As a result, horizontal polarization (in the direction $\perp\boldsymbol{g}$) of gyroscopic waves is far from circular at these latitudes, although gyroscopic wave polarization is always circular in their own plane of propagation. Also, vertical inertial currents are expected of the same order of magnitude as horizontal currents. This contrasts with near-inertial internal gravity waves supported by large stratification and thus demonstrating circular polarization in planes near-perpendicular to the gravity axis, i.e. near-parallel to the familiar Cartesian horizontal f-plane coordinates. For these waves, the vertical current is traditionally very small.

At intermediate stratification, the deviation angle from the direction of gravity is for $\alpha = \pi/2$ (LeBlond & Mysak 1978),

$$\nu = \arctan(\sin 2\varphi/(\cos 2\varphi + (N/2\Omega)^2))/2, \tag{A2}$$

which amounts to $\nu \approx 9°$ for rather weak $N = 2.5f$ at mid-latitudes (van Haren & Millot 2004), or relatively close to $\boldsymbol{g}$ still and well-away from $\boldsymbol{\Omega}$.

REFERENCES

ABARBANEL, H. D. I., HOLM, D. D., MARSDEN, J. E. & RATIU, T. 1984 Richardson number criterion for the nonlinear stability of three-dimensional stratified flow. *Phys. Rev. Lett.* **52**, 2352–2355.

COLIN DE VERDIÈRE, A. & SCHOPP, R. 1994 Flows in a rotating spherical shell: the equatorial case. *J. Fluid Mech.* **276**, 233–260.

GARGETT, A. E., HENDRICKS, P. J., SANFORD, T. B., OSBORN, T. R. & WILLIAMS III, A. J. 1981 A composite spectrum of vertical shear in the upper ocean. *J. Phys. Oceanogr.* **11**, 1258–1271.

GERKEMA, T. & SHRIRA, V. I. 2005*a* Near-inertial waves in the ocean: beyond the 'traditional approximation'. *J. Fluid Mech.* **529**, 195–219.

GERKEMA, T. & SHRIRA, V. I. 2005*b* Near-inertial waves on the 'nontraditional' β plane. *J. Geophys. Res.* **110**, C01003, doi:10.1029/2004JC002519.

GILL, A. E. 1982 *Atmosphere–Ocean Dynamics*. Academic.

VAN HAREN, H. 2006 Asymmetric vertical internal wave propagation. *Geophys. Res. Lett.* **33**, L06618, doi:10.1029/2005GL025499.

VAN HAREN, H. & MILLOT, C. 2004 Rectilinear and circular inertial motions in the Western Mediterranean Sea. *Deep-Sea Res. I* **51**, 1441–1455.

VAN HAREN, H. & MILLOT, C. 2006 Determination of buoyancy frequency in weakly stable waters. *J. Geophys. Res.* **111**, C03014, doi:10.1029/2005JC003065.

HOWARD, L. N. 1961 Note on a paper of John W. Miles. *J. Fluid Mech.* **10**, 509–512.

LEAMAN, K. D. & SANFORD, T. B. 1975 Vertical energy propagation of inertial waves: a vector spectral analysis of velocity profiles. *J. Geophys. Res.* **80**, 1975–1978.

LEBLOND, P. H. & MYSAK, L. A. 1978 *Waves in the Ocean*. Elsevier.

MARSHALL, J. & SCHOTT, F. 1999 Open-ocean convection: observations, theory, and models. *Rev. Geophys.* **37**, 1–64.

MILES, J. W. 1961 On the stability of heterogeneous shear flows. *J. Fluid Mech.* **10**, 496–508.

MILLOT, C. & CRÉPON, M. 1981 Inertial oscillations on the continental shelf of the Gulf of Lions – Observations and theory. *J. Phys. Oceanogr.* **11**, 639–657.

SAINT-GUILY, B. 1970 On internal waves. Effects of the horizontal component of the Earth's rotation and of a uniform current. *D. Hyd. Z.* **23**, 16–23.

SHEREMET, V. A. 2004 Laboratory experiments with tilted convective plumes on a centrifuge: a finite angle between the buoyancy and the axis of rotation. *J. Fluid Mech.* **506**, 217–244.

STRANEO, F., KAWASE, M. & RISER, S. C. 2002 Idealized models of slantwise convection in a baroclinic flow. *J. Phys. Oceanogr.* **32**, 558–572.